Acta Mech. Sin. (2011) 27(6):1065–1070
DOI 10.1007/s10409-011-0529-6

RESEARCH PAPER

Force–displacement characteristics of simply supported beam laminated with shape memory alloys

Zhi-Qiang Wu · Zhen-Hua Zhang

Received: 28 April 2010 / Revised: 1 November 2010 / Accepted: 30 December 2010

Abstract As a preliminary step in the nonlinear design of shape memory alloy (SMA) composite structures, the force–displacement characteristics of the SMA layer are studied. The bilinear hysteretic model is adopted to describe the constitutive relationship of SMA material. Under the assumption that there is no point of SMA layer finishing martensitic phase transformation during the loading and unloading process, the generalized restoring force generated by SMA layer is deduced for the case that the simply supported beam vibrates in its first mode. The generalized force is expressed as piecewise-nonlinear hysteretic function of the beam transverse displacement. Furthermore the energy dissipated by SMA layer during one period is obtained by integration, then its dependencies are discussed on the vibration amplitude and the SMA's strain (Ms-Strain) value at the beginning of martensitic phase transformation. It is shown that SMA's energy dissipating capacity is proportional to the stiffness difference of bilinear model and nonlinearly dependent on Ms-Strain. The increasing rate of the dissipating capacity gradually reduces with the amplitude increasing. The condition corresponding to the maximum dissipating capacity is deduced for given value of the vibration amplitude. The obtained results are helpful for designing beams laminated with shape memory alloys.

Keywords Shape memory alloy · Laminated beam · Bilinear hysteretic model · Force–displacement characteristics · Energy dissipation

1 Introduction

Shape memory alloys (SMA) have attracted more and more scholars' attentions due to their shape memory effect and pseudo-elasticity. They have been widely applied in mechanical engineering, civil engineering, aerospace engineering and so on [1–6]. At present, in the static and dynamic analysis of engineering structure, research on SMA composite structure mainly involves active and passive control of the deformation, vibration and noise of the beam and shell structure, of which the main composite structures adopted are: (1) SMA films are laminated with a substrate [6–10]; (2) SMA wires and alloying pellets are embedded into a substrate [11, 12]; (3) SMA fiber woven layer composite structures [13]. For the first laminated structure, the SMA is usually used as a surface, while the other elastic material is used as a substrate. Most of substrates are plate and a few of them are wave-shaped shell. The structures with plate substrate are reliable and easy to composite so that they are applied widely in deformation and noise control of beams and panels in engineering applications, and the results show that this composite structure can make full use of SMA's damping characteristics to achieve better vibration and deformation suppression effects [5–8,14,15].

Qin and Ren [16] studied dynamic response characteristics of SMA laminated simply supported beams. During vibration different points of its SMA layers may unload along different lines of SMA's pseudo-elasticity model. However,

The project was supported by the National Natural Science Foundation of China (10872142 and 10632040) and New Century Excellent Talents in University of China (NCET-05-0247) and the Key Program of the Natural Science Foundation of Tianjin (09JCZDJ26800).

Z.-Q. Wu (✉) · Z.-H. Zhang
School of Mechanical Engineering,
Tianjin University, 300072 Tianjin, China
e-mail: zhiqwu@tju.edu.cn

Z.-H. Zhang
Department of Electromechanical Engineering,
Nanyang Institute of Technology, 473004 Nanyang, China

this fact was not taken into account in their paper so that an important term was ignored in their model. A correct model will be developed in this paper.

The present paper consists mainly of four sections: Sect. 2 briefly describes the establishment and discretization of the dynamic partial differential equation of laminated beams which modifies the result in Ref. [16]; Sect. 3 carefully calculates the generalized restoring force caused in SMA layers by piecewise integration and analyzes the force–displacement characteristics, and similar work as this has not been found in present reports; Sect. 4 studies the energy dissipation capacity of SMA layers; and finally Sect. 5 discusses the results.

2 SMA laminated beam bending vibration model

2.1 SMA constitutive model

The present research uses the bilinear model (see Fig. 1) to express the superelasticity [17–19]. It had been shown by theoretical analysis and experimental verification that the model can meet engineering precision requirements. M_s and M_f in subscript represent, respectively, start and finish of the martensite transformation, while A_s and A_f represent the start and finish of the austensite transformation.

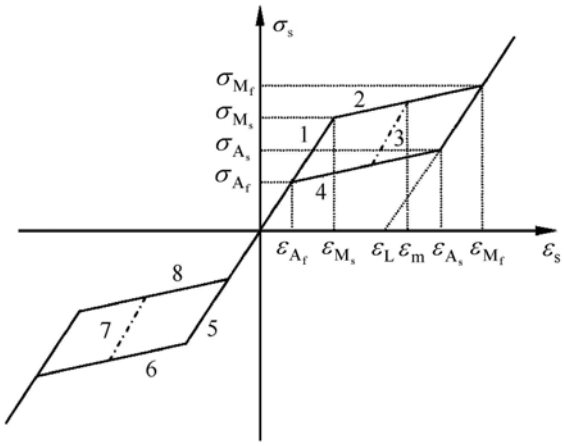

Fig. 1 SMA bilinear hysteresis loop constitutive model

The piecewise linear constitutive model is composed of 8 lines which are expressed in L_i ($i = 1, 2, \cdots, 8$) hereafter. L_1 and L_5 are linear elastic ranges in the SMA's austenitic state; L_2 and L_6 are SMA's martensite transformation ranges; L_3 and L_7 are the unloading ranges at the SMA incomplete martensite transformation state; L_4 and L_8 are the SMA's autensite transformation ranges. The relationship between SMA's strain and stress of L_i is expressed in unified form

$$\sigma_s = \sigma_{i0} + k_i \varepsilon_s = \sigma_{i0} + k_i \frac{\partial u_s}{\partial x}, \tag{1}$$

where

$$k_1 = k_3 = k_5 = k_7 = E_A,$$

$$k_2 = k_4 = k_6 = k_8 = \frac{\sigma_{M_f} - \sigma_{M_s}}{\varepsilon_{M_f} - \varepsilon_{M_s}},$$

$$\sigma_{10} = \sigma_{50} = 0,$$

$$\sigma_{20} = -\sigma_{60} = (k_1 - k_2)\varepsilon_{M_s},$$

$$\sigma_{30} = -\sigma_{70} = \sigma_{20} - (k_1 - k_2)\varepsilon_m,$$

$$\sigma_{40} = -\sigma_{80} = (k_1 - k_2)\varepsilon_{A_s}.$$

ε_m denotes the maximum strain of a point in the SMA material during the loading and unloading process. When the beam vibrates, the strain–stress states of the different points may be on different lines in Fig. 1. That is to say that the Eq. (1) is dependent on the axial position of a point on SMA layers.

2.2 Dynamics model of laminated beam

The SMA composite structure [8, 16] adopted here is shown in Fig. 2. SMA films are used as surface layers to make full use of the SMA damping characteristics. The middle substrate is made from linearly elastic material.

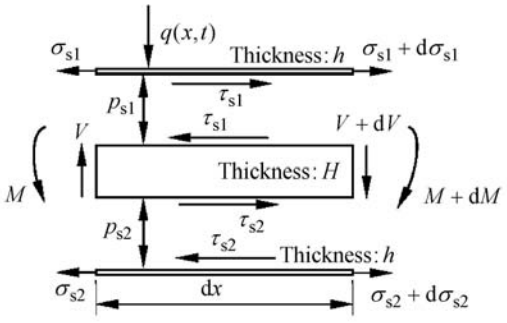

Fig. 2 Micro-unit mechanics model of laminated beam

Supposing that the beam span is long enough to meet the Euler-beam theory, the SMA layers are very thin and of equal thickness, meanwhile, there is no axial force in the beam. Then, by using the dynamic equilibrium equations of micro-unit, displacement coordination condition and deformation differential equation of the substrate, the dynamic equation of the substrate is obtained

$$m\frac{\partial^2 w}{\partial t^2} + c\frac{\partial w}{\partial t} + E_b\frac{bH^3}{12}\frac{\partial^4 w}{\partial x^4} + bhH\left[\frac{\partial^2 \sigma_0(x)}{\partial x^2} + \frac{(H+h)k(x)}{2}\frac{\partial^4 w}{\partial x^4}\right] = q(x,t), \tag{2}$$

where w is the deflection of the beam and its positive direction is downward. $\sigma_0(x) = \sigma_{i0}(x)$ and $k(x) = k_i(x)$ for all points x, whose strain–stress state, $(\varepsilon(x), \sigma(x))$ lies on line L_i ($i = 1, 2, \cdots, 8$) in Fig. 1. During vibration, the strain–stress states of different points of the SMA layers may be on different lines, therefore the model (Eq. (2)) is discontinuous on x,

while continuous but not smooth on t. Noted that, the term, $\sigma_0(x)$, has an important influence on the force–displacement characteristics and energy dissipation of SMA layers and can not be ignored [16]. Letting

$$\bar{x} = x/L, \qquad \bar{w} = w/L,$$
$$H_1 = h/H, \qquad H_2 = H/L,$$
$$\bar{k}_i = k_i/E_b, \qquad \bar{\sigma}_{i0} = \sigma_{i0}/E_b,$$
$$\bar{t} = t/t_0, \qquad t_0 = \sqrt{\frac{12Lm}{E_b b H_2^3}},$$
$$\bar{q}(\bar{x},\bar{t}) = \frac{12q(x,t)}{E_b b H_2^3}, \qquad \eta = \frac{ct_0}{m},$$

and substituting them into Eq. (2), gives the dynamics model in dimensionless form as follows

$$\frac{\partial^2 \bar{w}}{\partial \bar{t}^2} + \eta\frac{\partial \bar{w}}{\partial \bar{t}} + \frac{\partial^4 \bar{w}}{\partial \bar{x}^4} + \frac{12H_1}{H_2}\left[\frac{\partial^2 \bar{\sigma}_0(\bar{x})}{\partial \bar{x}^2} + \frac{(1+H_1)H_2\bar{k}(\bar{x})}{2}\frac{\partial^4 \bar{w}}{\partial \bar{x}^4}\right] = \bar{q}(\bar{x},\bar{t}). \quad (3)$$

If the beam is simply supported at both ends, then its deflection in the first mode can be expressed as

$$\bar{w} = \frac{-2}{\pi^2 H_2(1+H_1)} y \sin . \quad (4)$$

In this case, the strain distribution of the SMA layers is

$$\varepsilon_s = \frac{\partial \bar{u}_{s1}}{\partial \bar{x}} = \frac{H_2(1+H_1)}{2}\frac{\partial^2 \bar{w}}{\partial \bar{x}^2} = y(\bar{t})\sin(\pi\bar{x}), \quad (5)$$

where u_{s1} is the axial displacement of the upper SMA layer. It is obvious that $y(\bar{t})$ is the largest strain in the SMA layer.

Applying the Galerkin method to Eq. (3), one can obtain the single degree of freedom dynamic equation on $y(\bar{t})$

$$\frac{\partial^2 y(\bar{t})}{\partial \bar{t}^2} + \eta\frac{\partial y(\bar{t})}{\partial \bar{t}} + \pi^4 y(\bar{t}) + F_s = G, \quad (6)$$

where G and F_s, respectively, represent the generalized force caused by distributed loads and SMA layers. They are two integrations along the beam.

$$G = -\pi^2 H_2(1+H_1)\int_0^1 \bar{q}(\bar{x},\bar{t})\sin(\pi\bar{x})\mathrm{d}\bar{x},$$
$$F_s = 12\pi^2 H_1(1+H_1)F_s^0,$$

where

$$F_s^0 = \int_0^1 \left(\pi^2\bar{k}(\bar{x})y(\bar{t})\sin(\pi\bar{x}) - \frac{\partial^2\bar{\sigma}_0(\bar{x})}{\partial\bar{x}^2}\right)\sin(\pi\bar{x})\mathrm{d}\bar{x}. \quad (7)$$

The function $y(\bar{t})$ is denoted by y in the following sections for simplification.

3 Force–displacement characteristic of SMA layers

To express analytically the generalized restoring force F_s, it is only necessary to calculate the integration F_s^0 dependent on $\bar{x}$. This paper discusses the situation of $\varepsilon_{M_s} \le y_m \le \varepsilon_{M_f}$ where y_m denotes the maximum value of y. The vibration of the beam in half period can be divided into two processes, namely loading ($y: 0 \to y_m$) and unloading ($y: y_m \to 0$) which include two and four stages respectively. For all stages, the sections for different strain–stress states of SMA layers are shown in Fig. 3.

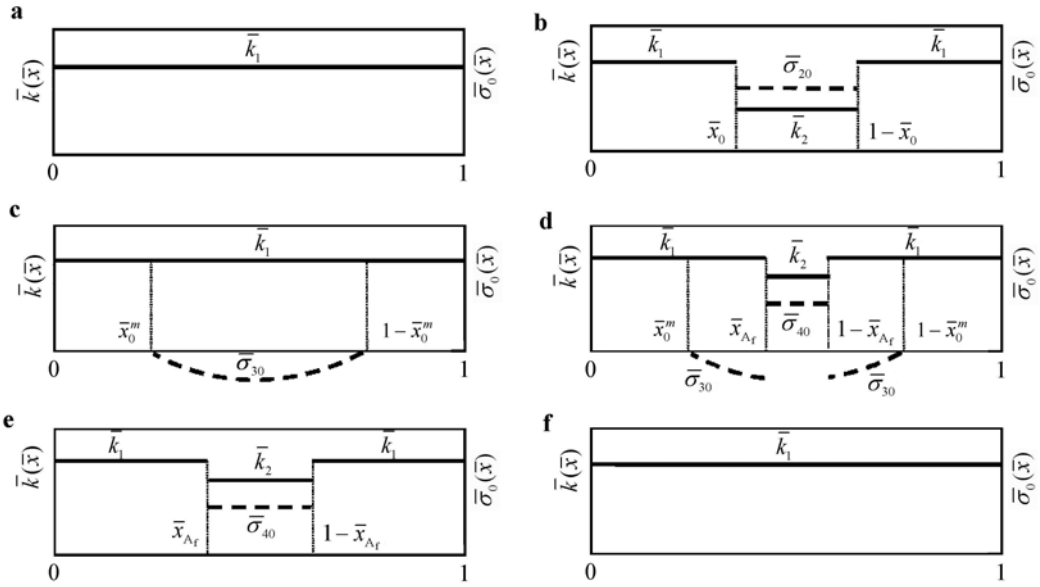

Fig. 3 Subsections of laminated beam at different deformation intervals ($\bar{k}(\bar{x})$ — solid line, $\bar{\sigma}_0(\bar{x})$ — dashed line). **a** $0 \le y < \varepsilon_{M_s}, \dot{y} > 0$; **b** $\varepsilon_{M_s} \le y < y_m, \dot{y} > 0$; **c** $y_1 < y \le y_m, \dot{y} < 0$; **d** $y_2 < y \le y_1, \dot{y} < 0$; **e** $\varepsilon_{A_f} \le y \le y_2, \dot{y} < 0$; **f** $0 \le y < \varepsilon_{A_f}, \dot{y} < 0$

The loading process is divided into two stages:

(1) $0 \le y < \varepsilon_{M_s}, \dot{y} > 0$ (Fig. 3a). All SMA in the beam is in elastic state of austenite

$$F_s^0 = \frac{1}{2}\pi^2 \bar{k}_1 y.$$

(2) $\varepsilon_{M_s} \le y < y_m, \dot{y} > 0$ (Fig. 3b): The SMA in section $(\bar{x}_0, 1-\bar{x}_0)$ is in martensitic transformation, while sections $[0, \bar{x}_0]$ and $[1-\bar{x}_0, 1]$ are still in the elastic state of the austenite phase. Here $\bar{x}_0$ meets $y\sin(\pi\bar{x}_0) = \varepsilon_{M_s}$. $\bar{x}_0$ decreases from $1/2$ to $\bar{x}_0^m$, when y increases from ε_{M_s} to y_m;

$$F_s^0 = \pi^2\left[\frac{\bar{k}_2}{2} + \bar{x}_0(\bar{k}_1 - \bar{k}_2)\right]y - \pi\cos(\pi\bar{x}_0)\varepsilon_{M_s}(\bar{k}_1 - \bar{k}_2).$$

The unloading process includes four stages:

(3) $y_1 < y \le y_m, \dot{y} < 0$ (Fig. 3c): In this stage, the three sections remain unchanged. SMA points in section $[\bar{x}_0^m, 1-\bar{x}_0^m]$ unload along lines parallel with L_3 with $\bar{\sigma}_{30} = (\bar{k}_1 - \bar{k}_2)(\varepsilon_{M_s} - y_m\sin(\pi\bar{x}))$, while points in other sections unload along L_1 with $\bar{\sigma}_0$ independent of $\bar{x}$. When $y = y_1 \triangleq y_m - (\varepsilon_{M_s} - \varepsilon_{A_f})$, the middle point first reaches line L_4

$$F_s^0 = \frac{\bar{k}_1\pi^2}{2}y + \frac{\pi}{2}(\bar{k}_1 - \bar{k}_2)(2\pi y_m\bar{x}_0^m - \pi y_m - 2\cos(\pi\bar{x}_0^m)\varepsilon_{M_s}).$$

(4) $y_2 < y \le y_1, \dot{y} < 0$ (Fig. 3d): The SMA in section. $(\bar{x}_1, 1-\bar{x}_1)$ are in austenite transformation where $\bar{x}_1$ meets $(y_m - y)\sin(\pi\bar{x}_1) = \varepsilon_{M_s} - \varepsilon_{A_f}$. When y decreases from y_1 to y_2, $\bar{x}_1$ decreases from $1/2$ to $\bar{x}_0^m$; Here $y_2 = \varepsilon_{A_f}y_m/\varepsilon_{M_s}$

$$F_s^0 = \left[\pi^2(\bar{k}_1 - \bar{k}_2)\bar{x}_1 + \frac{\pi^2\bar{k}_2}{2}\right]y - \pi(\bar{k}_1 - \bar{k}_2)[y_m\pi(\bar{x}_1 - \bar{x}_0^m) + \cos(\pi\bar{x}_0^m)\varepsilon_{M_s} - \cos(\pi\bar{x}_1)(\varepsilon_{M_s} - \varepsilon_{A_f})].$$

(5) $\varepsilon_{A_f} \le y \le y_2, \dot{y} < 0$ (Fig. 3e): The austenite transformation section $[\bar{x}_{A_f}, 1-\bar{x}_{A_f}]$ reduces from $[\bar{x}_0^m, 1-\bar{x}_0^m]$ to the middle point of the beam, where $\bar{x}_{A_f}$ meets $y\sin(\pi\bar{x}_{A_f}) = \varepsilon_{A_f}$

$$F_s^0 = \pi^2\left[\frac{\bar{k}_2}{2} + \bar{x}_{A_f}(\bar{k}_1 - \bar{k}_2)\right]y - \pi\cos(\pi\bar{x}_{A_f})\varepsilon_{A_f}(\bar{k}_1 - \bar{k}_2).$$

(6) $0 \le y < \varepsilon_{A_f}, \dot{y} < 0$ (Fig. 3f): The SMA in whole beam comes to the austensite state again

$$F_s^0 = \frac{1}{2}\pi^2\bar{k}_1 y.$$

It is easy to see that the generalized restoring force F_s is hysteretic and nonlinear about y (see Fig. 4a). If the term $\bar{\sigma}_{30}$ is ignored as paper [16], F_s curves fail to be closed (see Fig. 4b). That is why $\sigma_0(x)$ can not be omitted in Eqs. (2) and (3).

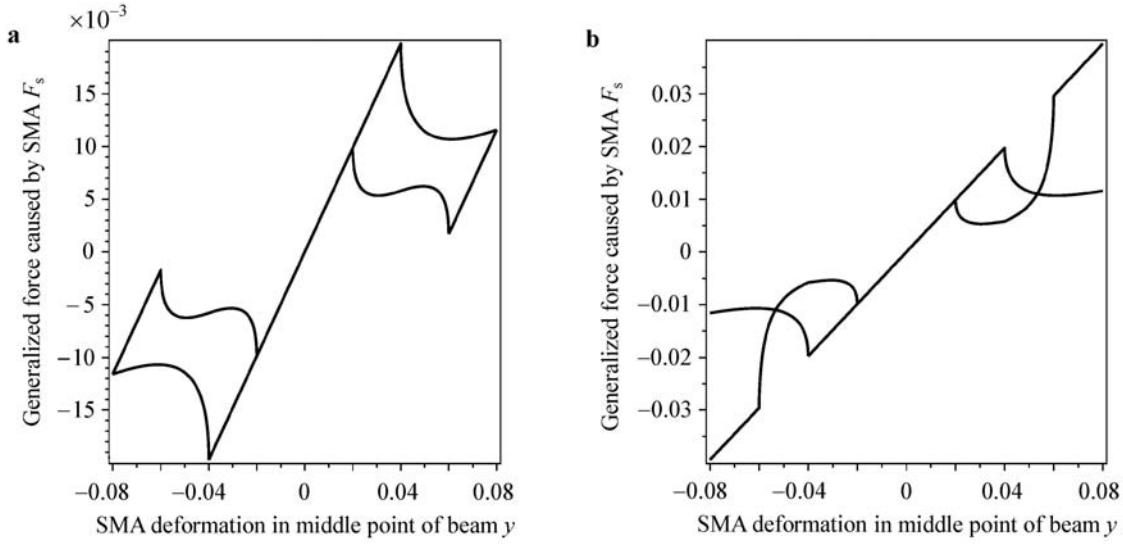

Fig. 4 The hysteresis relationship between SMA generalized force and deformation of beam

4 Influence of phase transformation parameters on energy dissipation capacity

When $y_m \ge \varepsilon_{M_s}$, SMA layers dissipate energy during beam vibration. In the case where $y_m \le \varepsilon_{M_f}$, the energy dissipated in one period equals the area summation A of two hysteresis loops as given below

$$A = 2\left\{\int_{\varepsilon_{A_f}}^{\varepsilon_{M_s}} \frac{\pi^2}{2}\bar{k}_1 y\,dy + \int_{\varepsilon_{M_s}}^{y_m}\left\{\pi^2\left[\frac{\bar{k}_2}{2} + \bar{x}_0(\bar{k}_1 - \bar{k}_2)\right]y - \pi\cos(\pi\bar{x}_0)\varepsilon_{M_s}(\bar{k}_1 - \bar{k}_2)\right\}dy - \int_{y_1}^{y_m}\left\{\frac{k_1\pi^2}{2}y + \frac{\pi}{2}(\bar{k}_1 - \bar{k}_2)[2\pi y_m\bar{x}_0^m - \pi y_m\right.$$

$$-2\cos(\pi\bar{x}_0^m)\varepsilon_{M_s}]\Big\}dy - \int_{y_2}^{y_1}\Big\{\Big[\pi^2(\bar{k}_1-\bar{k}_2)\bar{x}_1+\frac{\pi^2\bar{k}_2}{2}\Big]y$$

$$-\pi(\bar{k}_1-\bar{k}_2)[y_m\pi(\bar{x}_1-\bar{x}_0^m)+\cos(\pi\bar{x}_0)\varepsilon_{M_s}$$

$$-\cos(\pi\bar{x}_1)(\varepsilon_{M_s}-\varepsilon_{A_f})\Big]\Big\}dy$$

$$-\int_{\varepsilon_{A_f}}^{y_2}\Big\{\pi^2\Big[\bar{x}_{A_f}(\bar{k}_1-\bar{k}_2)+\frac{\bar{k}_2}{2}\Big]y$$

$$-\pi\varepsilon_{A_f}\cos(\pi\bar{x}_0^A)(\bar{k}_1-\bar{k}_2)\Big\}dy\Big\}$$

$$=4\pi\varepsilon_{M_s}\frac{k_1-k_2}{E_b}(\varepsilon_{M_s}-\varepsilon_{A_f})$$

$$\times\Big[\frac{\pi}{2}-\arcsin\Big(\frac{\varepsilon_{M_s}}{y_m}\Big)\Big]. \tag{8}$$

It is obvious that the energy dissipation capacity is proportional to k_1-k_2 and $\varepsilon_{M_s}-\varepsilon_{A_f}$ for fixed ε_{M_s}. Thus choosing SMA materials with a larger value of the two differences is better for damping elements. In the following the effect on energy dissipation of the two important parameters, y_m and ε_{M_s}, is discussed.

(1) y_m and A

The relationship between y_m and A is as shown in Fig. 5 for other fixed parameters, which suggests the area of hysteresis loop increases as y_m increases, but the increasing ratio decreases.

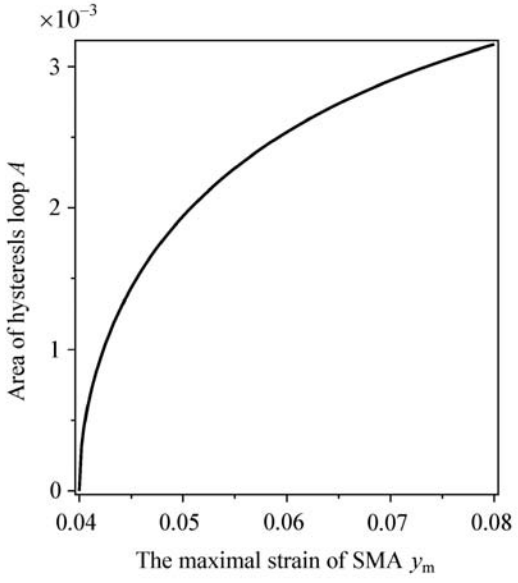

Fig. 5 The relationship between area of hysteresis loop and the maximal strain at the midpoint of beam

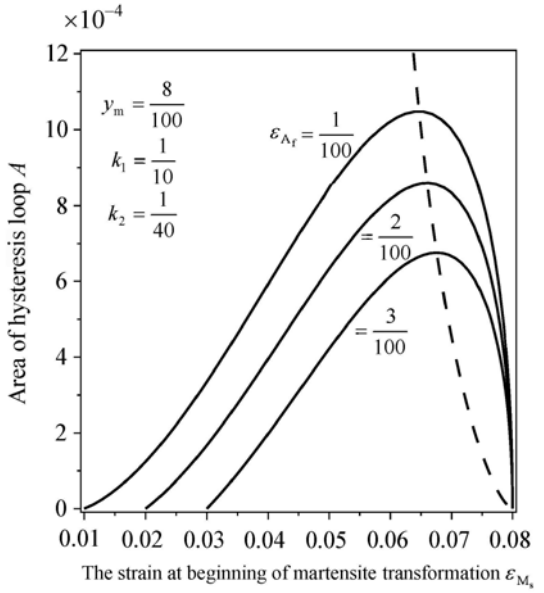

Fig. 6 The relationship between area of hysteresis loop and phase transformation parameter of SMA

(2) ε_{M_s}, ε_{A_f} and A

The effects of the two parameters, ε_{M_s}, ε_{A_f} are shown in Fig. 6 for other fixed parameters. A is not monotonic on ε_{M_s} with a maximum value in the investigated interval and increasing as ε_{A_f} decreases.

From the equation $\dfrac{\partial A}{\partial\varepsilon_{M_s}}=0$, one can find out the extremum condition

$$\eta=2\xi\Big\{1+\frac{\xi}{[\sqrt{1-\xi^2}(\pi-2\arcsin\xi)-2\xi]}\Big\}, \tag{9}$$

in which $\eta=\varepsilon_{A_f}/y_m$, $\xi=\varepsilon_{M_s}/y_m$, noting that $0<\eta<\xi<1$. When Eq. (9) is satisfied, A reaches its maximum, A_{max}, which is given below and plotted as a dashed line in Fig. 6

$$\frac{A_{max}}{4\pi(\bar{k}_1-\bar{k}_2)}=y_m^2\xi\Big[\frac{\xi^2}{\xi-\sqrt{1-\xi^2}(\pi/2-\arcsin\xi)}-\xi\Big]$$

$$\times\Big(\frac{\pi}{2}-\arcsin\xi\Big). \tag{10}$$

The above analysis suggests that the area of hysteresis loop can achieve the maximum when the phase transformation parameters meet a certain relationship (9). That is to say that the perfect damping effect can be obtained through choosing SMA material with suitable parameters.

5 Conclusions

The SMA laminated beam simply-supported at both ends is investigated in this paper. The main results are listed as follow.

(1) To build up the correct model for laminated beam vibration, the terms, describing the influence of intercepts of lines in a piecewise constitutive relationship of the SMA, must be included.
(2) The generalized force caused by SMA layers presents a piecewise nonlinear characteristic instead of a piecewise linear one for the strain–stress relationship in the SMA constitutive model.
(3) The energy dissipation of the SMA increases as the strain amplitude increases, and is proportional to the difference between the two stiffness's of the SMA bilinear model. In addition, for a given amplitude, energy dissipation of the SMA can achieve maximum value if the SMA's phase transformation parameters satisfy a certain relationship.

References

1 Sreekumar, M., Singaperuma, M.: A generalized analytical approach to the coupled effect of SMA actuation and elastica deflection. Smart Materials and Structures **18**, 1–15 (2009)
2 Casciati, F., Faravelli, L., Al Saleh, R.: An SMA passive device proposed within the highway bridge benchmark. Structural Control and Heath Monitoring **16**, 657–667 (2009)
3 Johnson, R., Padgett, J.E., Maragakis, M.E., et al.: Large scale testing of nitinol shape memory alloy devices for retrofitting of bridges. Smart Materials and Structures **17**, 1–10 (2008)
4 Sreekumar, M., Nagarajan, T., Singaperumal, M.: Application of trained NiTi SMA actuators in a spatial compliant mechanism: Experimental investigations. Materials and Design **30**, 3020–3029 (2009)
5 Hartl, D.J., Lagoudas, D.C.: Aerospace applications of shape memory alloys. Proceedings of the Institution of Mechanical Engineers-Journal of Aerospace Engineering **221**, 535–552 (2007)
6 Roh, J.H., Lee, I., Han, J.H.: Damping characteristics of SMA films and their application for passive vibration isolation. International Journal of Applied Electromagnetics and Mechanics **27**, 225–241 (2008)
7 Balapgol, B.S., Bajoria, K.M., Kulkarni, S.A.: Natural frequencies of a multilayer SMA laminated composite cantilever plate. Smart Materials and Structures **15**, 1021–1032 (2006)
8 Chen, Q., Levy, C.: Active vibration control of elastic beam by means of shape memory alloy layers. Smart Materials Structures **5**, 400–406(1996)
9 Sepiani, H., Ebrahimi, F., Karimipour, H.: A mathematical model for smart functionally graded beam integrated with shape memory alloy actuators. Journal of Mechanical Science and Technology **23**, 3179–3190 (2009)
10 Ogisu, T., Shimanuki, N., Kiyoshima, S.: Damage suppression in CFRP laminates using embedded shape memory alloy foils. Advanced Composite Materials **13**, 27–42 (2004)
11 Qiu, Z., Yao, X., Jiang, Y.: Experimental research on strain monitoring in composite plates using embedded SMA wires. Smart Materials and Structures **15**, 1047–1053 (2006)
12 Ren, Y., Sun S.: Large amplitude flexural vibration of the orthotropic composite plate embedded with shape memory alloy fibers. Chinese Journal of Aeronautics **20**, 415–424 (2007) (in Chinese)
13 Zhang, R., Ni, Q.: Vibration characteristics of laminated composite plates with embedded shape memory alloys. Composite Structures **74**, 389–398 (2006)
14 Lua, T.J., Hutchinson, J.W., Evans, A.G.: Optimal design of arexural actuator. Journal of the Mechanics and Physics of Solids **49**, 2071–2093 (2001)
15 Elzey, D.M., Sofla, A.Y.N., Wadley, H.N.G.: A shape memory-based multifunctional structural actuator panel. International Journal of Solids and Structures **42**, 1943–1955 (2005)
16 Qin, H.Z., Ren, Y.S.: Frequency response characteristics of vibration of flexible beam covered with shape memory alloy (SMA) layers. Journal of Mechanical Strength **24**, 045–048 (2002)(in Chinese)
17 Du, X.W., Sun, G., Sun, S.S.: Piecewise linear constitutive relation for pseudo-elasticity of shape memory alloy (SMA). Materials Science and Engineering A **393**, 332–337 (2005)
18 Motahari, S.A., Ghassemieh, M.: Multilinear onedimensional shape memory material model for use in structural engineering applications. Engineering Structures **29**, 904–913 (2007)
19 Wagner, M.F.X., Eggeler, G.: Stress and strain states in a pseudoelastic wire subjected to bending rotation. Mechanics of Materials **38**, 1012–1025 (2006)